Supplemental Data

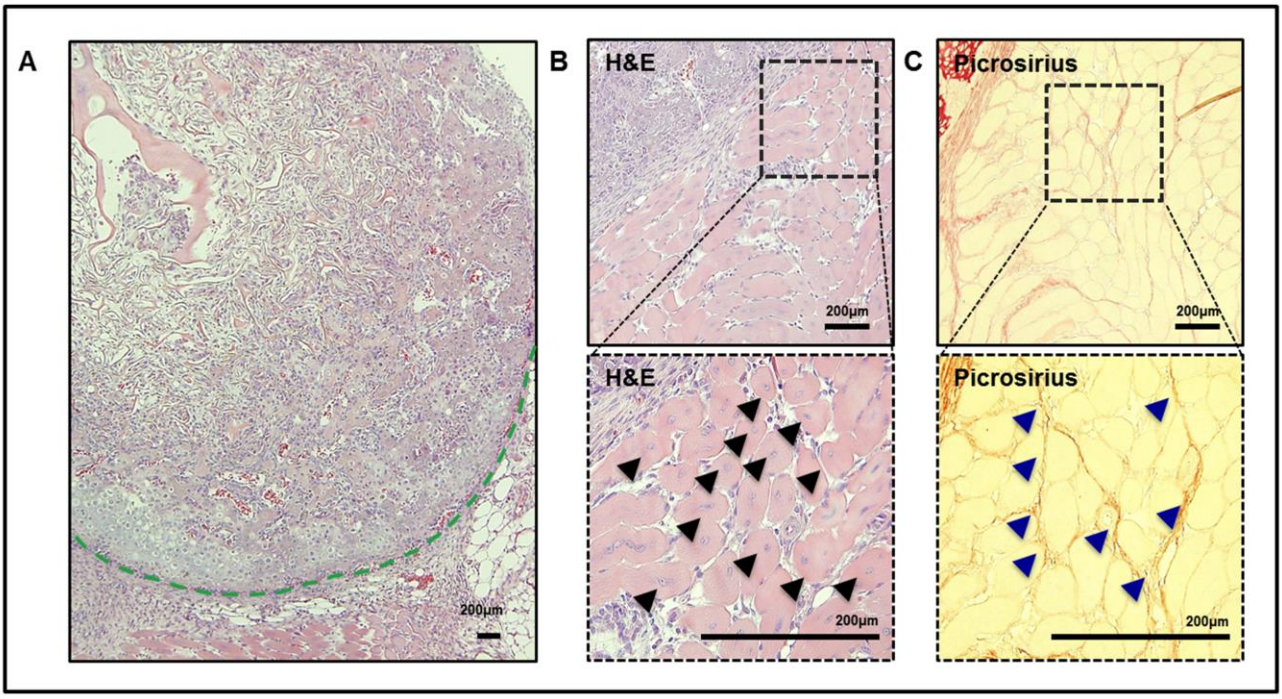

Fig S1. Intramuscular BMP ossicle implantation with concomitant cardiotoxin injury causes surrounding myofiber damage and fibrosis. (A) Ectopic bone at the site of BMP ossicle and cardiotoxin placement (green line demarcates border of ectopic bone); (B) Myofiber damage located outside of the ectopic bone (black arrowheads indicate centralized nuclei); (C) Areas of fibrosis corresponding to myofiber damage in (B) indicated by picrosirius red (blue arrowheads indicate picrosirius staining). All scale bars = 200 um.

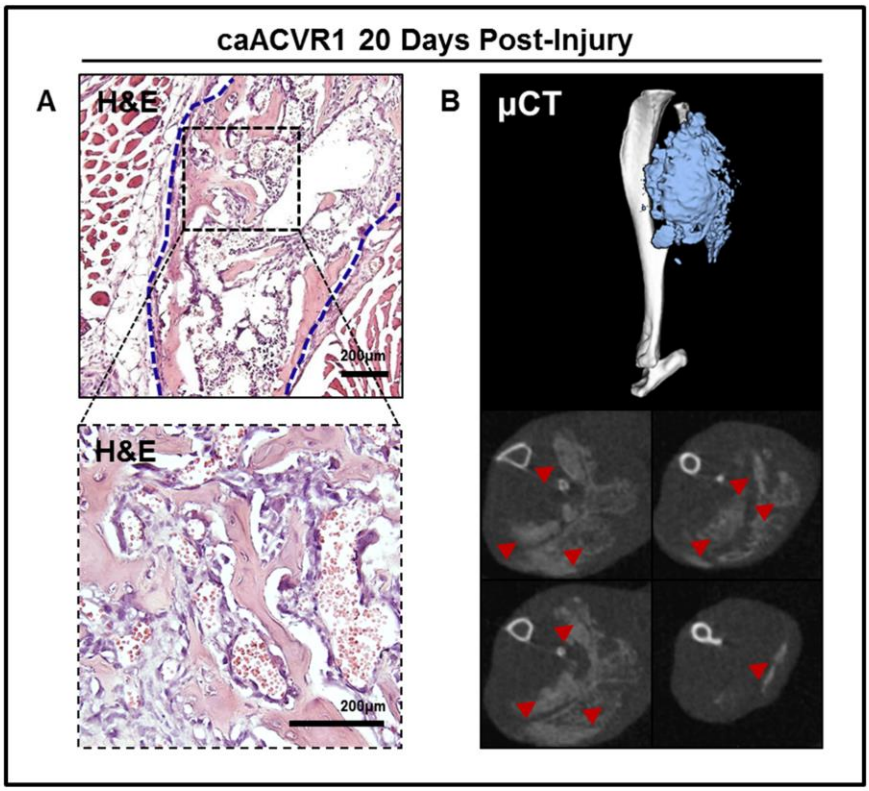

Fig S2. Intramuscular ectopic bone in a model of hyperactive BMP signaling with cardiotoxin injury. (A) H&E showing ectopic bone in gastrocnemius muscle of *caAcvr1*$^{fl/fl}$ mice 20 days after Ad.cre/CTX (adenoviral cre and cardiotoxin) injury; (B) MicroCT confirming presence of ectopic bone (blue) on 3-D reconstruction and serial cross-sections (red arrowheads). All scale bars = 200 um.

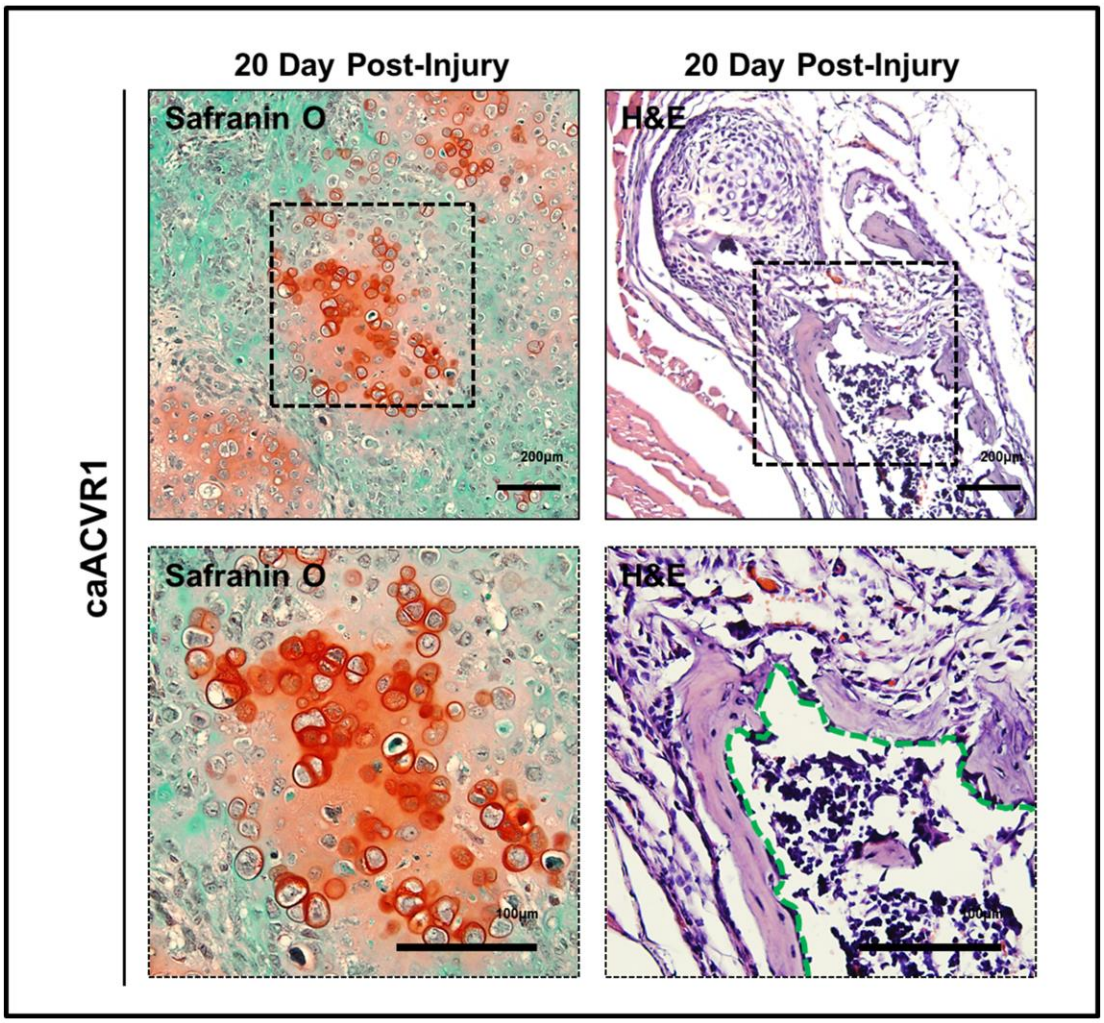

Fig S3. Intramuscular bone formation in caACVR1$^{fl/fl}$ mice is an endochondral process. Histologic staining of heterogenous intramuscular HO regions in *caAcvr1*$^{fl/fl}$ mouse, demonstrating cartilage formation with Safranin O staining (red), and woven bone with developing marrow space (green outline) by H&E staining, indicating HO formation is a dynamic and endochondral process.

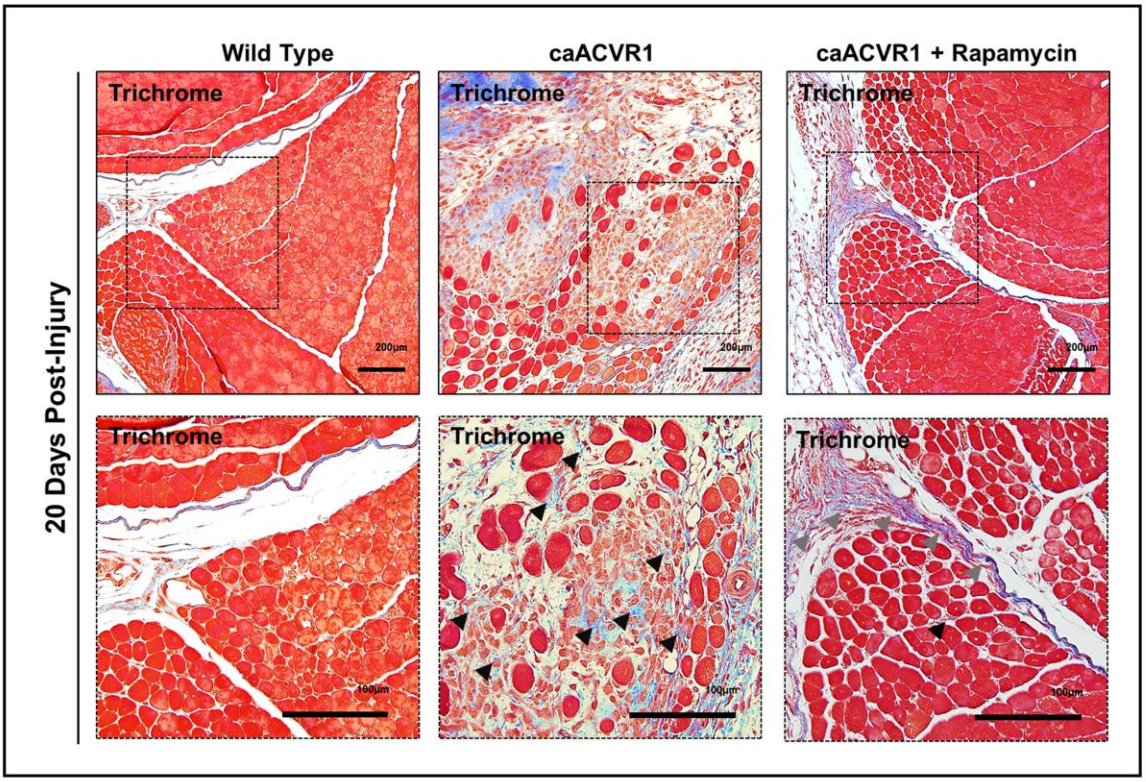

Fig S4. Rapamycin attenuates collagen deposition induced by activation of caACVR1$^{fl/fl}$ mutation.

Trichrome staining of wild-type, mutant *caAcvr1*$^{fl/fl}$, and mutant mice treated with rapamycin 20 days following Ad.cre/CTX injury, demonstrating intramuscular deposition in mutant mice, and resolution with rapamycin treatment.

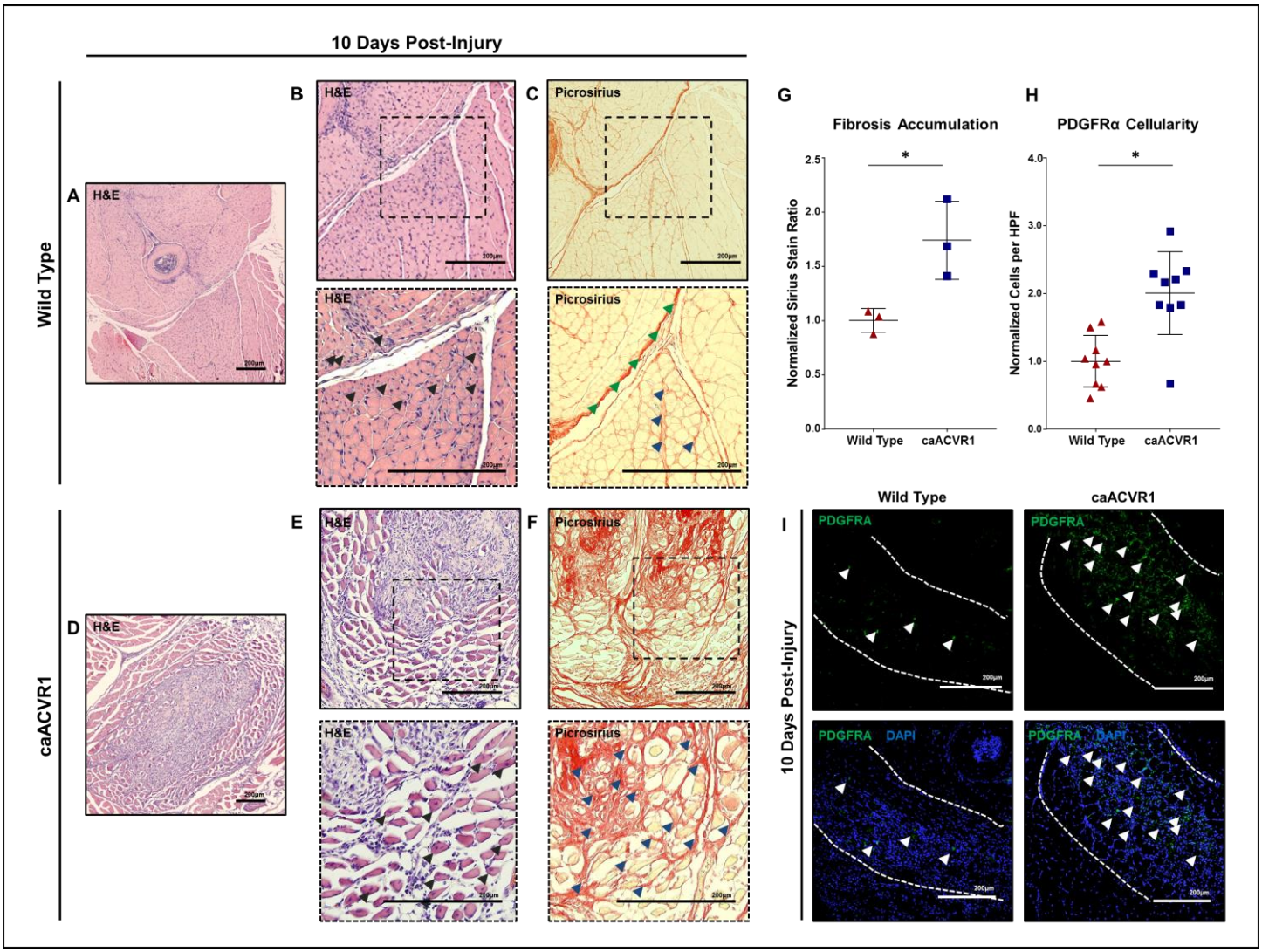

Fig S5. Myofiber injury and fibrosis precede the osseous lesion in *caACVR1$^{fl/fl}$* mice 10 days after Ad.cre/CTX injury. (A) Absence of ectopic bone in wild-type hindlimb 10 days after Ad.cre/CTX-injury; (B) Area of myofiber injury with centralized nuclei in wild type mice 10 days after injury (black arrowheads indicate myofibers with centralized nuclei); (C) Fibrosis corresponding with regions of myofiber injury (green arrowheads indicate fascial plane; blue arrowheads indicate fibrosis); (D) Absence of ectopic bone in *caACVR1$^{fl/fl}$* mouse 10 days after Ad.cre/CTX-injury; (E) Area of myofiber injury with centralized nuclei in mutant mice 10 days after injury (black arrowheads indicate myofibers with centralized nuclei); (F) Fibrosis corresponding with regions of myofiber injury (blue arrowheads indicate fibrosis); (G) Increased fibrosis staining based on picrosirius in *caAcvr1$^{fl/fl}$* mice when compared with wild type mice 10 days after Ad.cre/CTX injury (normalized ratio: 1.74 v. 1.0, n=3, student's two-tailed T-Test $p<0.05$); (H) Increased accumulation of mesenchymal cells (PDGFRA) at injury site of *caACVR1$^{fl/fl}$* mice when compared with wild type mice 10 days

after Ad.cre/CTX injury (normalized ratio: 2.0 v. 1.0, n=8, students two-tailed T-Test, $p<0.05$); (I) Representative immunostaining for PDGFRA in wild type and *caACVR1*$^{fl/fl}$ mice 10 days after Ad.cre/CTX injury (white arrowheads indicate PDGFRA+ cells; white dashed line demarcates area of fibrosis and myofiber injury). All scale bars = 200 um. *$p<0.05$.

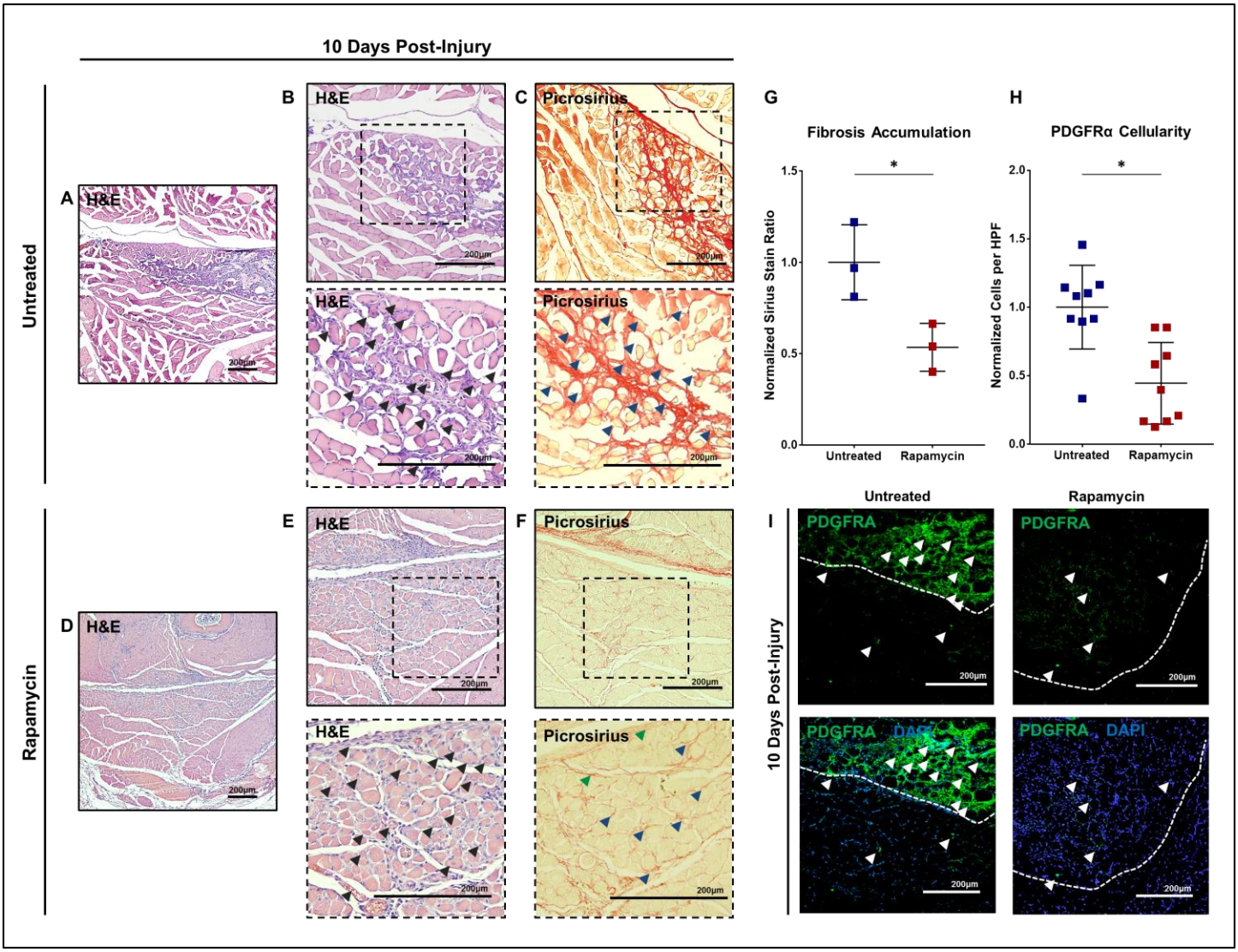

Fig S4. **Rapamycin eliminates fibrosis associated with hyperactive BMP signaling early after injury.** (A) Absence of ectopic bone in untreated and rapamycin-treated *caACVR1*$^{fl/fl}$ mice 10 days after Ad.cre/CTX (adenoviral cre and cardiotoxin injury); (B) Area of myofiber injury with centralized nuclei in untreated *caACVR1*$^{fl/fl}$ mice 10 days after Ad.cre/CTX injury (black arrowheads indicate myofibers with centralized nuclei); (C) Fibrosis corresponding with regions of myofiber injury in untreated *caAcvr1*$^{fl/fl}$ mice 10 days after Ad.cre/CTX injury (blue arrowheads indicate fibrosis); (D) Absence of ectopic bone in the hindlimb of rapamycin-treated *caACVR1*$^{fl/fl}$ mice 10 days after Ad.cre/CTX injury; (E) Area of myofiber injury with centralized nuclei in rapamycin-treated *caACVR1*$^{fl/fl}$ mice 10 days after Ad.cre/CTX injury (black arrowheads indicate myofibers with centralized nuclei); (F) Fibrosis corresponding with regions of myofiber injury in rapamycin-treated *caACVR1*$^{fl/fl}$ mice 10 days after Ad.cre/CTX injury (blue arrowheads indicate fibrosis); (G) Quantification confirms reduction in fibrosis in areas of muscle injury (normalized ratio: 0.52 v. 1.0, n=3, student's two-tailed T-Test, $p<0.05$); (H) Quantification confirms reduction in mesenchymal cells (PDGFRA) in areas of muscle injury (normalized ratio: 0.44 v. 1.0, n=8, students two-tailed T-Test, $p<0.05$); (I) Representative immunostaining for PDGFRA in untreated and rapamycin-treated, *caACVR1*$^{fl/fl}$ mice 10 days after Ad.cre/CTX injury. All scale bars = 200 um. *$p<0.05$.

Supplemental Fig 7. Fibroblasts harvested from caACVR1$^{fl/fl}$ mice exhibit increased osteogenesis in vitro. ALP staining of fibroblasts harvested from caACVR1$^{fl/fl}$ mice treated with control (Ad.Control) and Ad.Cre virus respectively. Spectroscopy quantification staining demonstrating increased osteogenic activity in Ad.Cre treated cells (normalized staining intensity, 6.15 v. 1, n=3, student's two-tailed T-Test, $p < 0.05$).

Table One: Reported complications associated with surgical use of rhBMP2 implants										
	All Events		**Inflammation**		**Infection**		**HO**		**Pain**	
	n	**%**	**n**	**%**	**n**	**%**	**n**	**%**	**n**	**%**
With Inflammation	1698	16.5	1698	100	372	48.4	620	39.0	1469	24.2
With Infection	768	7.5	372	21.9	768	100	119	7.5	577	9.5
With HO	1588	15.5	620	36.5	119	15.5	1588	100	1468	24.2
With Pain	6071	59.2	1469	86.5	577	75.1	1468	92.4	6071	100

Table 1. Reported adverse events associated with surgical use of rhBMP2 implants, compiled from the Manufacturer and User Facility Device Experience (MAUDE) Database.